Windmill Torque Estimation of Spin-type Solar Sail with Shape Control

J. Kikuchi(Tokyo Univ.), T. Chujo (Tokyo Univ.), T. Mizumori (Tokai Univ.), Y. Shirasawa(JAXA), O. Mori(JAXA)

Solar Sail Demonstrator "IKAROS" has been successful in a technology demonstration in space. During the period of the operation, the pictures taken by the monitor cameras revealed that the sail became an unexpected shape because of a curving of the thin-film solar cells. It was also confirmed that "windmill behavior" which constantly reduces the spin rate of the sail. In this study, it is suggested that the control method of the windmill torque with the shape control evens out the range of curving of thin-film solar cells. In addition, the control method is evaluated by comparing a geometrical estimation and a simple FEM analysis.

形状制御を用いたスピン型ソーラーセイルの風車トルク推定

菊池隼仁（東大・院）、中条俊大（東大・院）、水森主（東海大・院）、白澤洋二（JAXA）、森治(JAXA)

2010年5月に打ち上げられた小型ソーラー電力セイル実証機"IKAROS"はマストを要しないスピン型ソーラーセイルタイプであり、世界で初めて宇宙空間での技術実証に成功した。IKAROS 運用時、薄膜太陽電池の反り効果により膜面形状は予測がされていない形状に変形しており、セイル本体のスピン軸が傾く"渦巻き運動"や、膜面形状に依存してスピンレートが変動する"風車トルク"と呼ばれる現象が発生することが確認された。本研究では、ソーラーセイルの形状を制御することにより、薄膜太陽電池の反りの効果範囲内であっても発生する風車トルク値のコントロールを可能とする手法を提案し、風車トルク値の簡易 FEM 解析結果と幾何学形状推定を比較することで同手法の評価を行う。

Nomenclature

F	=	inertial force of element
K	=	spring constant
α	=	compression ratio
β	=	attenuation coefficient
L	=	distance between particles
L_0	=	natural distance between particles
ε	=	total distortion
B	=	strain displacement conversion
u	=	displacement vector of element
u_A	=	directional vector of element A
u_B	=	x directional vector of element B
v_B	=	y directional vector of element B
x_A	=	x directional displacement of element A
x_B	=	x directional displacement of element B
y_B	=	y directional displacement of element B
σ	=	stress vector
D	=	stress strain conversion matrix
E	=	Young's modulus
ν	=	Poisson coefficient
V	=	volume of element
K	=	spring constant vector
t	=	thickness of sail
S	=	area of triangle element
δ_i	=	displacement of element
f_i	=	direction force of element i
k_i	=	spring constant of element i
F_i	=	inertial force of element i

I. Introduction

A solar sail is a spacecraft which can make the altitude control and solar power generation possible by deploying a thin-film in space. Recently, the technology of the solar sail is actively researched. Solar Sail Demonstrator IKAROS (Fig.1), which was launched on May 21, 2010 was a successful technology demonstration. The main successes are as follows: First, deployment of a large sail membrane; second, generation of electricity by thin-film solar cells; third, demonstration of photon propulsion; fourth, demonstration of guidance, navigation and control techniques for solar sail propulsion.

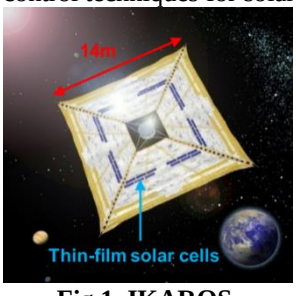

Fig.1 IKAROS

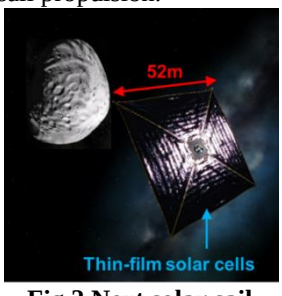

Fig.2 Next solar sail

IKAROS is a spinning type solar sail equipped with a large solar sail that is kept extended by the centrifugal force generated by the spinning of the spacecraft. To be compared with a mast type, it is possible to design a lightweight when the scale of the

sail becomes big. In contrast, because the solar sail deploys by only using a centrifugal force and the sail shape depends on the spin rate, it is difficult to estimate the sail shape. Initially, the stretched shape of IKAROS was expected to be a flat shape. But the pictures taken by the monitor cameras revealed that the sail took an unexpected shape because of a curving of the thin-film solar cells. Besides on, IKAROS exhibited unexpected attitude behaviors that were considered to be due to SPR effects caused by the nonflat and nonuniform sail surfaces. After the sail deployment, the spin axis of the sail body inclines and starts to circle. This motion is considered to be due to the SRP torque acting on the sail. Therefore, this motion is referred to as "spiral behavior" (Fig.3) of the spin axis. Another behavior can be confirmed in the spin rate. After the sail deployment, the spin rate of IKAROS is reduced. It is also considered to occur due to the SRP torque acting on the sail. This phenomenon and the torque are termed "windmill behavior" and "windmill torque". (Fig.4)

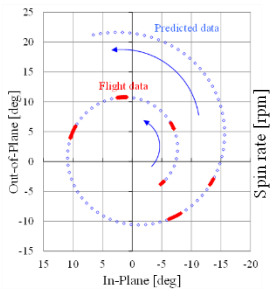

Fig.3 Spiral behavior (Oct. 18 – Oct. 29, 2011)

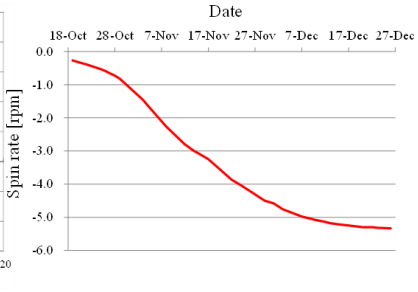

Fig.4 Windmill behavior (Oct. 18 – Dec. 26, 2011)

For IKAROS and future spin type solar sails, the spiral behavior and the windmill behavior, which are difficult motions to estimate the direction, have a negative influence on the operation. Because the next solar sail will be equipped thin-film solar cells on the entire surface and designed to be a large scale, the effect of the spiral behavior and the windmill behavior increases more than IKAROS. However, it is difficult to mount a fuel consumed in order to fix it under severe weight request. In this study, it is suggested that the control method of the windmill torque with the shape control evens in the range of curving of thin-film solar cells.

II. Analysis Configuration

IKAROS is connected to four trapezoidal membranes of which the length of outer circumference is 14m. (Fig.5) A trapezoidal membrane is called a petal in this paper. In order to deploy the sail by using the centrifugal force of the spin, it is equipped with four tip masses of 0.5kg in each tip interval of the petals. After deployment, the sail keeps the stretched shape by continuing to spin at 1rpm as nominal spin rate. In this study, following configuration is used, which has improved the problems that have been discovered in IKAROS as shown below.

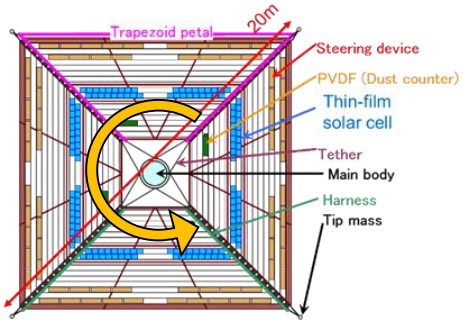

Fig.5 IKAROS Configuration

A. Tether arrangement

For the purpose of enhancing the safety of the sail deployment, a tether arrangement is performed to increase the attenuation of the deployment. In order to decrease the outer plane vibration, four tether divided into upper and lower per petal are respectively connected to the body. It also functions to suppress in-plane vibration by connecting the tether at a crossing point of the body and at two vertices of the trapezoid petals (Fig.6). However, in the case of the tether arrangement, because the tether is not arranged in a straight line to the trapezoidal hypotenuse, it would work in the direction of the force due to the tether shrinking circumferentially the petal during the spin. As a result, it has a disadvantage that it is impossible to maintain a flat shape. Therefore, this model has been designed to reduce the deformation by changing the model tether trapezoidal hypotenuse as being arranged in a straight line.

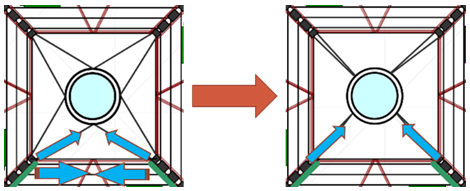

(a)IKAROS **(b)Analysis model**

Fig.6 Plane tether arrangement

B. Curve of solar cell

For the purpose of providing a tension to the tether even if it has manufacturing errors, an artificially deformation margin of the sail circumferentially called "circumferential margin" is provided in IKAROS. For example, if the manufacturing error of the tether is longer or the sail size is smaller than the design, the tether does not have a tension and becomes slack. In this case, a dead zone (Fig.7), which is the area where the sail does not follow the spin of the body, occurs in

the sail. If the dead zone is generated, it is considered that it is impossible to control the attitude of the sail well. As a result, it has a negative influence on the operation. Therefore, in order to have a tension inside the tether, it is given the circumferential margin, which the sail can deform in the circumferential direction by increasing the area of the apparent sail by changing artificially the mounting position of the bridge and the sail. As a result, it makes it possible that the tether always has a tension and prevents the occurrence of the dead zone.

However, it can be confirmed from the analysis of the image captured by a camera mounted on IKAROS (Fig.8), that the tether is slack and has no tension. For the main reason, thin-film solar cells are curved in the direction in which they shrink to the circumferential direction of the sail in space. As a result, the circumferential margin is completely absorbed and the tethers become slack. The thin-film solar cells mounted on the next solar sail are currently developed for the suppression and the management of curving.

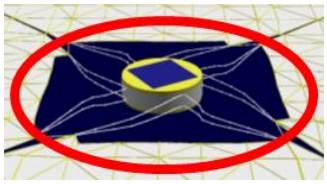

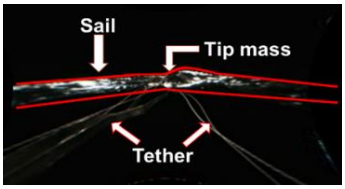

Fig.7 Dead zone **Fig.8 pictures taken by cameras**

C. Tip mass arrangement

IKAROS has four tip masses, which are set in each sail vertex (Fig.9 Left). This arrangement has a feature that the movement of every petal would be linked to each other because the direction of the centrifugal force is only in one way. In contrast, it is possible to control the independent movement of the petals by separating into two tip masses at each vertex in this model (Fig.9 Right). Since the centrifugal force is also separated in two directions as well, it is possible to affect an inclination of the sail to the outer side well. Therefore, it has a positive influence of generating the windmill torque.

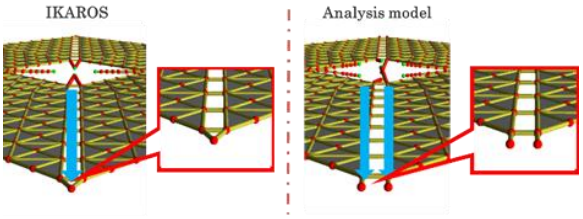

Fig.9 Tip mass arrangement

D. Windmill torque control

The tethers are connected completely symmetrical in the z-axis direction in the conventional design (Fig.10 Left). In this case, there are no geometric factors that determine the direction of the windmill torque. For this reason, the estimation of the windmill torque is complicated. Therefore, the analysis model changes to have an inclination in petals artificially, by providing a gap height in the body connecting part of the tether, which are connected from each vertex of the inner side of trapezoid petals (Fig.10 Right). As a result, an active control of the direction of the windmill torque becomes possible.

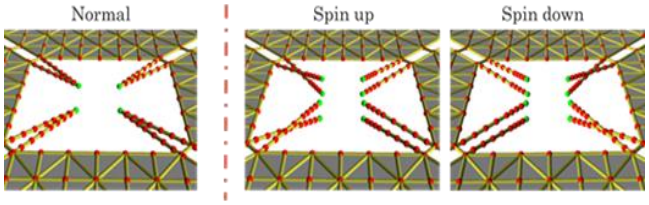

(a)Normal **(b)Direction control**

Fig.10 Tether arrangement

III. Analysis Method

A. Simple FEM analysis

The simple FEM used in this study is an improved one of multi-particle method (MPM). The sail is defined as a mass point, a spring and a damper in MPM. It is possible to significantly reduce the long calculation time required in the FEM analysis of thin-film structures. The windmill torque is calculated by assuming that a solar radiation pressure (SRP) is given from 0° sun angle to the center of gravity of each triangular face from making three particles. Therefore, the force acting between particles is obtained with the following equation:

$$\mathrm{F} = \begin{cases} K(L - L_0) + \beta K\dot{L}(L \geq L_0) \\ K\alpha(L - L_0) + \alpha\beta K\dot{L}(L < L_0) \end{cases} \quad (1)$$

MPM has a disadvantage that it cannot simulate the effect of the displacement in one direction given in other directions because it represents the spring constant as a diagonal matrix from the approximation of the three directions. By contrast, Simple FEM allows to reflect an influence of the displacement in all directions to the sail by assuming that it is also including a component in the triangle shape. When u_A, u_B, v_B are defined as the displacement of elements, ε and B can be calculated as follows:

$$\boldsymbol{\varepsilon} = \mathbf{Bu} = \mathbf{B}\begin{bmatrix} u_A \\ u_B \\ v_B \end{bmatrix} \quad (2)$$

$$\mathbf{B} = \begin{bmatrix} \frac{1}{x_A} & 0 & 0 \\ 0 & 0 & \frac{1}{y_B} \\ -\frac{x_B}{x_A y_B} & \frac{1}{y_B} & 0 \end{bmatrix} \quad (3)$$

By assuming elements of an isotropic material sail, the relationship between σ and D is obtained as follows from the theoretical strength of materials.

$$\boldsymbol{\sigma} = \mathbf{D}\boldsymbol{\varepsilon} = \boldsymbol{D}\begin{bmatrix}\varepsilon_x \\ \varepsilon_y \\ \gamma_{xy}\end{bmatrix} \tag{4}$$

$$\mathbf{D} = \frac{E}{1-\nu^2}\begin{bmatrix}1 & \nu & 0 \\ \nu & 1 & 0 \\ 0 & 0 & \frac{1-\nu}{2}\end{bmatrix} \tag{5}$$

By assuming that the displacement of the vertex, which corresponded to F, is matched to $\mathrm{u} = (u_A\ u_B\ v_A)^T$, the equation of the external force and the internal one on the sail can be represented as follows:

$$(\mathrm{du})^T\boldsymbol{F} = \int d\varepsilon^T\boldsymbol{\sigma}dV \tag{6}$$

$$\mathbf{F} = (\int \boldsymbol{B^T D B}dV)\mathrm{u} = \mathbf{Ku} \tag{7}$$

Assuming the sail thickness is a uniform from (2)-(5), K can be represented as follows:

$$\mathbf{K} = \int \boldsymbol{B^T D B}dV \approx \boldsymbol{B^T D B}tS \tag{8}$$

$$= \frac{tE}{2(1-\nu^2)}\begin{bmatrix}\frac{y_B}{x_A} + \frac{1-\nu}{2}\frac{{x_B}^2}{x_A y_B} & -\frac{1-\nu}{2}\frac{x_B}{y_B} & \nu \\ -\frac{1-\nu}{2}\frac{x_B}{y_B} & \frac{1-\nu}{2}\frac{x_A}{y_B} & 0 \\ \nu & 0 & \frac{x_A}{y_B}\end{bmatrix} \tag{9}$$

From the theory, MPM is calculated with the equation of the motion only by displacement in one direction. But it is possible to reflect the equation of the motion displacement in all directions in Simple FEM. As a result, a simulation of a strict model can be performed.

Table1. Comparison of MPM and Simple FEM

MPM	Simple FEM
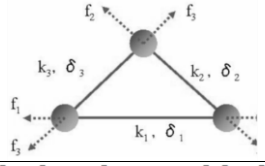	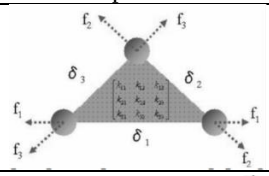
$\begin{bmatrix}F_1\\F_2\\F_3\end{bmatrix} = \begin{bmatrix}k_1 & & \\ & k_2 & \\ & & k_3\end{bmatrix}\begin{bmatrix}\delta_1\\\delta_2\\\delta_3\end{bmatrix}$	$\begin{bmatrix}F_1\\F_2\\F_3\end{bmatrix} = \begin{bmatrix}k_{11} & k_{12} & k_{13}\\ k_{21} & k_{22} & k_{23}\\ k_{31} & k_{32} & k_{33}\end{bmatrix}\begin{bmatrix}\delta_1\\\delta_2\\\delta_3\end{bmatrix}$
Diagonal matrix	Symmetric matrix

B. Analysis configuration

Taking into account that it will be compared with the experimental analysis in the future, this analysis used the model of the sail in a thirtieth scale rather than the actual size of IKAROS. The model has eight circumferential sides and maintaining the spin rate of 3Hz. In order to investigate the effect of the windmill torque by a shape control, it is assumed that an external force such as gravity and SRP is not taken into consideration. The gap height to control the windmill torque in the body provides 12mm.

Since the next solar sail has mounted thin-film solar cells to the whole petals, this analysis has also adopted the same configuration model (Fig.11). The tether arrangement is adopted by the method shown in Fig.10. Three types can be analyzed: spin up, spin down and normal. Tip mass arrangement is also adopted by the method shown in Fig.9. In order to simulate a force for curving the solar cells, a rotational spring constant is introduced, which is proportional to the curve angle. In order to analyze the relationship between the circumferential margin and each curve angle of the solar cells, this analysis is performed by changing parameters in the curve angle in the range of 0° to 48°. The decreasing of the circumferential margin can be confirmed as the curve angle increases because the outer side of the sail amounts to a larger area of the solar cells than the inner one.

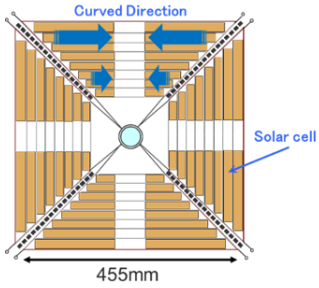

Fig.11 Analysis configuration

C. Geometrical estimation

In order to propose a method of estimating the windmill torque, it is calculated from the geometrical shape of the sail and compared with the result of Simple FEM. Simple FEM calculates the windmill torque by assuming that a SRP is given from 0° sun angle to the center of the gravity of each triangular face and maintaining the spin rate of 3Hz. On the other hand, Geometrical estimation calculates by assuming that the petals are a planar shape and there is no spin rate. The SRP works from 0° sun angle to the center of the gravity of each petal. Therefore, Geometrical estimation has lower accuracy than Simple FEM.

Table 2. Comparison of Simple FEM analysis and Geometrical estimation

	Simple FEM analysis	Geometrical estimation
Spin rate	3Hz	No consideration
Calculation	Each triangular face	Each petal
Accuracy	Higher	Lower

Fig.12 shows the result of the windmill torque in response to the curve angle by Geometrical estimation. The petal has a twist angle under the influence of the tether arrangement. Since the circumferential length decreases by the curving of the solar cells, the twist angle of the petal also decreases as well. Because each circumferential side has a different twist angle, the windmill torque also generates a different value depending on each circumferential side. Therefore, the windmill torque reaches a maximum when the twist angle of the petal is the same as the innermost circumferential side. On the other hand, it reaches a minimum when the twist angle is the same as the outermost one. The several curves in Fig.12 show the windmill torque of Geometrical estimation when the twist angle is assumed from First side (the innermost) to Eighth side (the outermost). From these estimations, it can be predicted that the result of the windmill torque in Simple FEM is between the minimum and the maximum of Geometrical estimation.

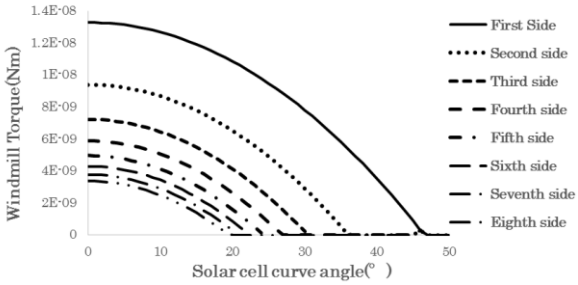

Fig.12 Windmill torque of Geometrical estimation

IV. Analysis Result

A. Direction control

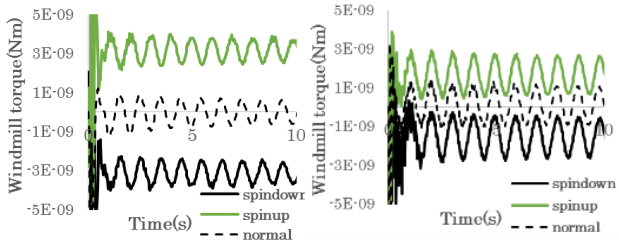

(a) Curve angle 0° **(b) Curve angle 24°**

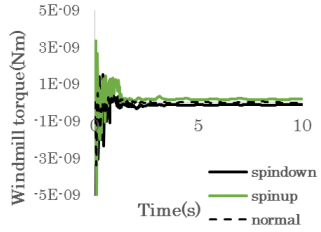

(c)Curve angle 48°

Fig.13 Windmill torque comparison in each tether arrangement

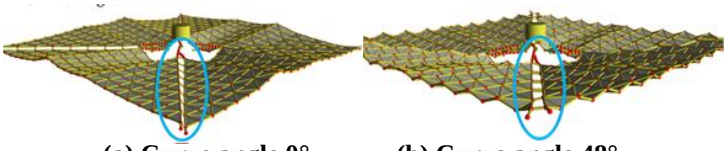

(a) Curve angle 0° **(b) Curve angle 48°**

Fig.14 Comparison of sail twist in each angle

Fig. 13 shows a time transition of the windmill torque for each curve angle when the tether arrangement is placed spin up, spin down and normal. From the analysis results, it can be confirmed that it is possible to control the direction of the windmill torque by changing the tether arrangement in the range of 0°~24° of the curve angle. On the other hand, it also can be confirmed that there is almost no generation of the windmill torque in 48° curve angle. Therefore, the windmill torque gradually decreases as the curve angle increases. As the factor from the images of Simple FEM(Fig.14),because the length of the circumferential direction of the sail also decreases as the curve angle increases, the twist angle of the petal that generates the windmill torque also decreases. Therefore, the windmill torque also decreases accordingly.

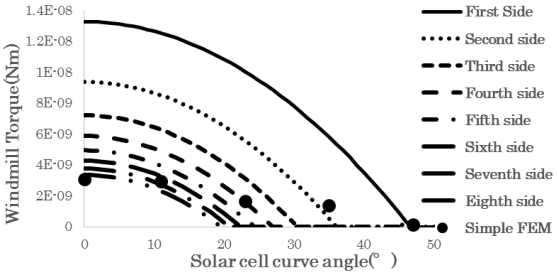

Fig.15 Windmill torque comparison of Geometrical estimation and Simple FEM analysis

The five points shown in Fig.15 are plots of the average value of the windmill torque for each curve angle. To be compared with Geometrical estimation, the result of Simple FEM follows the windmill torque of the eighth side (the outermost) of Geometrical estimation. It can be considered as following two main factors: 1. The outer side has a bigger area reflecting a SRP than the inner one. 2. Because the arm length of the outer side is longer than the inner one, the windmill torque also increases in proportion. From this two reasons, the effect of the outer side is dominant in determining the windmill torque.

Geometrical estimation is also expected to generate no windmill torque in 48° of the curve angle. The result of Simple FEM is also consistent with this estimation. If the curve angle becomes nearly 48°, the twist angle of the petal would be completely offset. For this reason, it is impossible to control the direction of the windmill torque. Therefore, in order to control the windmill torque, it is necessary to keep a minimum curve angle of the solar cells.

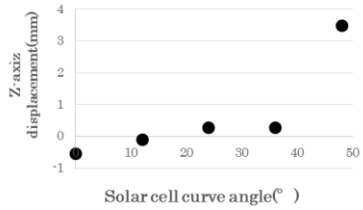

Fig. 16 Z-axis displacement of sail vertex particles

Fig.16 shows a comparison for each z-axis displacement of the particles of the sail vertex in each curve angle from the main body. The z-axis displacement takes the value of nearly 0 mm. Therefore the sail shape is a relatively flat in the range of 0°~36° of the curve angle. By contrast, the particles rise in the direction of the z-axis in 48° of the curve angle. It indicates that the center of gravity of the sail also rises. As this factor, the curving of the solar cells completely offsets the twist angle of the sail when it reaches 48° of the curve angle. As a result, the tether does not have any tensions and starts to become slack. Therefore, because the tether has a margin to move in the z-axis direction, the entire sail can also rise. From these results, the twist angle of the sail functions of the circumferential margin in this analysis model. On the other hand, if the curve angle excesses the constant angle, the disadvantage of not being able to control the windmill torque appears.

B. Application of a different scale sail

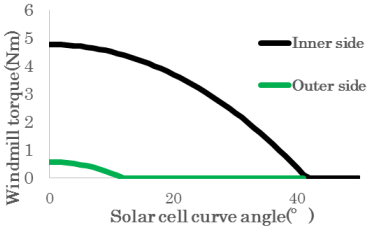

Fig.17 Windmill torque estimation of next solar sail

Fig.17 shows an estimation of the windmill torque in the configuration of the next solar sail by Geometrical estimation. The next solar sail will be a model which has the solar cells attached to the entire petals as in the present analytical model. The scale is that the inner side is 6 m and outer side is 52 m. The gap height to control the windmill torque in the body provides 500mm. From the analysis results, it is possible to generate the windmill torque up to nearly 40° of the curve angle in the innermost side.

For this reason, the windmill torque of the next solar sail also can be controlled up to nearly 40° of the curve angle. Therefore, if the scale of the solar sail becomes any size, the direction, the value of the windmill torque and the range of the acceptable curve angle of the solar cells can be estimated by using Geometrical estimation.

V. Conclusion

In this study, it is suggested that the control method of the windmill torque with the shape control evens out the range of curving of the thin-film solar cells. In addition, the control method is also evaluated by comparing Geometrical estimation and Simple FEM.

This analysis configuration has adopted following changes, which has improved the problems that have been discovered in IKAROS. First, this model is designed to reduce the deformation of the sail by changing the tether arrangement. Second, it is possible to affect an inclination of the sail to the outer side by separating into two tip masses at each vertex. Third, the analysis model changes to have an inclination in petals artificially by providing a gap height. As a result, an active control of the direction of the windmill torque becomes possible. From the analysis results, it can be clearly confirmed that it is possible to control the direction of the windmill torque by changing the tether arrangement. But if the twist angle of the sail decreases because of curving of the solar cells, it is impossible to control the direction of the windmill torque. Therefore, in order to prevent generating a dead zone, it is necessary to keep to a minimum angle of the solar cells.

The comparison of Simple FEM and Geometrical estimation is also investigated. The result of Simple FEM follows the windmill torque of the outermost side of Geometrical estimation. As a result, the effect of the outer side is dominant in determining the windmill torque value. From this comparison, if the scale of the solar sail becomes any size, the direction, the value of the windmill torque and the range of the acceptable curve angle of the solar cells can be estimated by using Geometrical estimation.

References

[1] Yuichi Tsuda, “Improved Multi-Particle Model for Dynamics Analysis of Arbitrary-Shaped Thin Flexible Structure”, Workshop on Astrodynamics and Flight Mechanics, Vol.14, A-2, 2004, pp 7-12

[2] Yuich Tsuda, Osamu Mori, “Dynamics Analysis of Solar Sail Membrane Using Improved Multi-Particle Model”, Workshop on Astrodynamics and Flight Mechanics, Vol.15, B-3, 2005, pp 160-166

[3] Yoji Shirasawa ”Study on the effect of Bending Stiffness on the Membrane Dynamics of Solar Power Sail Demonstrator “IKAROS””, American institute of Aeronautics and Astronautics, 2008, pp.1-11

[4] Toshihiro Chujo, Y. Tsuda, and T. Saiki, “Solar Sail Attitude Dynamics Considering Sail Deformation”, AAS Space Flight Mechanics Meeting, AAS13-759, Hilton head, 2013